Time evolution of ZnO-CNT photoluminescence under variable ambient and temperature conditions

IOP Conf. Series: Materials Science and Engineering **613** (2019) 012031 doi:10.1088/1757-899X/613/1/012031

Time evolution of ZnO-CNT photoluminescence under variable ambient and temperature conditions

P Rauwel[1], A Galeckas[2] and E Rauwel[1]

[1]Institute of Technology, Estonian University of Life Sciences, Kreutzwaldi 56/2, Tartu (Estonia)
[2]Department of Physics, University of Oslo. P.O. Box 1048 Blindern, 0316 Oslo (Norway)

Email: protima.rauwel@emu.ee

Abstract. ZnO-CNT hybrid materials were prepared by non-aqueous sol-gel routes at 240ºC. The morphology and defects have been studied by transmission electron microscopy and photoluminescence spectroscopy. The hybrid nanostructures manifest a broad luminescence emission covering the visible spectrum. Variations in photoluminescence with time are observed for the ZnO-CNT hybrid structures exposed to different ambient and temperatures. The studies show that photoluminescence from adsorbed oxygen dominates the emission emanating from other intrinsic defects and also affects the stability of the latter over time.

1. Introduction

ZnO and carbon-nanotube (CNT) hybrid materials have gained popularity over the past decades [1, 2] which is largely due to the influence that the carbon-based component exerts over the synthesis of ZnO nanoparticles, hence in determining the ultimate properties. In its general bulk form, ZnO is a semiconductor material with a wide band gap of 3.37eV, however, once the crystal dimensions are reduced to the nanometer scale, the presence of carbon-based materials can modify the crystallinity, defect states as well as the morphology of the ZnO nanoparticles (NPs). In turn, the photoluminescence (PL) of such hybrid structures is also modified as compared to the stand-alone ZnO NPs. Typical PL spectrum of ZnO exhibits two characteristic features - a relatively narrow peak in the UV region pertaining to the near-band-edge (NBE) emission and originating from exciton annihilation and recombination processes via shallow states [3, 4]. The other characteristic feature is a broad visible emission originating from intrinsic defects that introduce luminescent states within the band gap, hence commonly referred to as deep-level emission (DLE) band. The intensity ratio of NBE to DLE allows for qualitative assessment of the crystallinity of ZnO. The ZnO-CNT hybrid structures generally yield a high NBE to DLE ratio due to an enhanced surface plasmon mediated effect [5]. Also noteworthy is that the presence of carbon-based structures has a photocatalytic effect on ZnO, as it introduces defect states in the band gap of ZnO which then serve as efficient photoexcited charge separators [6].

Besides the ZnO NPs crystallinity, an equally important characteristic is the stability of the hybrid material properties, which can be assessed by monitoring the developments of luminescence properties over time under continuous UV exposure at different ambient and temperature conditions. In the case of ZnO-CNT hybrid structures, the time evolution of PL features to a large extent reflects the stability of the defects involved; these include point and surface defects of the ZnO as well as the interfacial defects between the ZnO and CNT. The charging effects of the surface states, their passivation and the energy transfer efficiency from ZnO to CNT along with the presence of impurities and defect sites, all these

factors can introduce significant variations in the charge carrier dynamics over time. In this regard, time-lapse PL measurements may provide an insight into the charge developments which is essential for determining the feasibility of ZnO–CNT hybrid structures in optoelectronic applications.

In the present work, we extend further our earlier studies of PL in air and in vacuum [7] and focus on the charge carrier behavior over time by monitoring time evolution of the PL features of ZnO-CNT hybrid structures prepared via a non-aqueous sol gel route at 240ºC. Such an approach provides insights into the origin of luminescent states within the bandgap and their stability at different temperatures (10K and 300K) and ambient conditions (vacuum and air), which are among the key factors in determining the potential of these hybrid nanostructures in optoelectronic applications.

2. Experimental

2.1 Synthesis

The procedure for synthesizing ZnO NPs was carried out under air. In a typical synthesis, zinc acetate (3.41mmol) (99.99%, Aldrich) was added to 20 mL (183mmol) of benzylamine (≥99.0%, Aldrich). The reaction mixture was transferred into a stainless steel autoclave and carefully sealed. Thereafter, the autoclave was taken out of the glovebox and heated in a furnace at a temperature 240°C for 2 days. The resulting milky suspensions were centrifuged; the precipitates were thoroughly washed with ethanol and dichloromethane and subsequently dried in air at 60°C. In the case of the carbon nanohybrid synthesis, NANOCYL NC7000 MWCNT with an average diameter of 10nm and length of 1.5μm was used. For the synthesis of carbon-based ZnO nanocomposites, the MWCNTs were directly homogeneously dispersed into the solution of zinc acetate and benzylamine before transferring the solution into an autoclave for the reaction synthesis.

2.2 Characterization:

High-resolution transmission electron microscopy (HRTEM) was carried out on a probe-corrected Titan G2 80− 200kV operating at 200kV in TEM mode and providing a point to point resolution of 2.4Å. Photoluminescence (PL) measurements were carried out at 10K and 300K temperatures by employing the 325 nm wavelength of a cw He− Cd laser with an output power of 10mW as an excitation source. The emission was collected by a microscope and directed to a fiber optic spectrometer (Ocean Optics USB4000, spectral resolution 2 nm). Temperature dependent measurements were realized using closed-cycle He-refrigerator (Janis, Inc. CCS450). Room temperature PL measurements of the powder-like samples have been performed both in air and vacuum. The density of the compact powders is estimated to be approximately the same in all measurements.

3. Results and discussions

3.1 Morphological characterizations

Former x-ray diffraction studies demonstrated that ZnO nanoparticles are highly crystalline with a hexagonal wurtzite ($P6_3mc$) crystal structure (a = 3.25Å and c = 5.20Å) with an average diameter of 90nm [7]. The TEM image of figure 1 provides an overview of the nanoparticles synthesized at 240ºC. ZnO particles of various shapes are illustrated. The nanotubes visible at the center of the image are linked to various ZnO particles, showing an intimate contact between them. The shape of the nanoparticle is an indication of the presence of polar surfaces in such materials. Hexagonal shaped nanoparticles contain 4 non-polar surfaces and 2 polar surfaces, where the former type is susceptible to oxygen vacancies and therefore also oxygen chemisorption [8]. The HRTEM study showed that the size of the ZnO nanoparticles is around 125nm. The arrows indicate strain in the ZnO structure implying stacking faults in the volume of the nanoparticle.

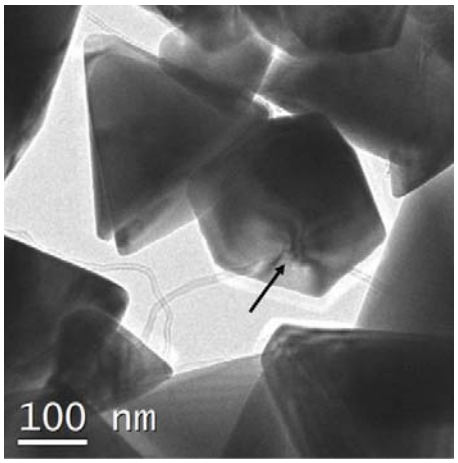

Figure 1. TEM image of ZnO-CNT synthesized at 240ºC

3.2 Photoluminescence characterization

The time evolution of the ZnO-CNT photoluminescence was investigated as a function of different ambient (air versus vacuum) and temperature (room versus cryogenic) conditions. Figures 2, 3 and 4 summarize the time-lapse PL measurements with the key elements of emission represented by Gaussian deconvolution fits. One can observe a certain similarity of all PL plots featuring a repeatable set of the same key spectral components, as indicated by vertical markers positioned at around 3.1eV, 2.8eV, 2.5eV, 2.3eV, 2.1eV and 1.9eV. Another shared feature is a significant decrease of the PL intensity in the visible blue-green regions of spectra with the elapsed UV-exposure time. The dynamics of this process for each particular case of ambient and temperature is represented by a characteristic decay time constant (τ) estimated from the integrated PL intensity transients shown in the insets of figures 2, 3 and 4.

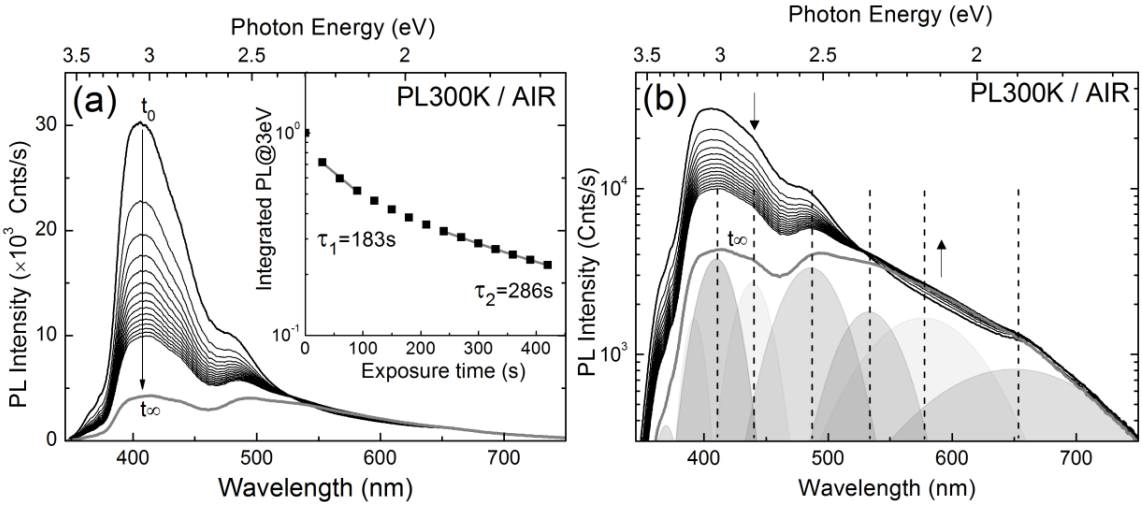

Figure 2. Time evolution of the PL measured at 300K in air ambient from the hybrid ZnO-CNT nanocomposites synthesized at 240ºC: (a) time-lapse PL spectra as a function of UV-exposure time. Inset shows decay transient of the integrated PL intensity. (b) Semi-log plot of the PL developments with the key spectral components represented by Gaussian deconvolution fits (shaded areas); vertical dashed markers indicate the monitored spectral components; up/downward arrows point out PL intensity trends.

The dominant feature in all presented PL spectra is a broad blue band combining conventional NBE emission with two extra components at 3.1eV and 2.8eV, which are within spectral region known for

optical manifestation of zinc vacancies (V_{Zn}) and interstitials (Zn_i) [9, 10]. The NBE emission adjoins and partially overlaps with the deep-defect related green luminescence comprised of two closely positioned bands centered at 2.3eV and 2.5eV. The latter, at 2.5eV, occurs when a singly ionized oxygen vacancy turns neutral (V_O^+/ V_O) on capturing an electron from the conduction band and recombining with a valence band hole [11]. The other green emission component at 2.3eV is believed to originate from a singly ionized surface oxygen vacancy capturing a hole from the surface states and turning doubly ionized (V_O^+/ V_O^{2+}), thus largely representing a surface phenomenon unlike the green emission at 2.5eV which is mostly volume-related. Finally, the red emission centered at 1.9eV is commonly attributed to accumulation of zinc vacancies, as separate V_{Zn} clusters or in association with extended defects, and apparently remains unchanged over time under any of varied ambient conditions (cf. figures 2, 3 and 4). The presence of the extended defects is directly evidenced by TEM image in figure 1, thus supporting the relation of the red emission with the accumulated V_{Zn} point defects.

Figure 2 shows PL of the hybrid ZnO-CNT measured in air ambient at 300K as a function of UV-exposure time. One can observe a substantial (~10 fold) and rapid PL intensity decrease (decay times 183s/286s) in the UV-visible spectral region. The underlying mechanism behind this dynamic phenomenon is attributed to surface band bending induced by adsorbents and their gradual desorption stimulated by UV-illumination. The actual band bending is a superposition of several opposed effects expected from trapping of H_2O and O_2 molecules, from hydroxyl (OH) termination or some residual surface contaminants. For ZnO-CNT hybrids prepared by non-aqueous route at 240ºC, the most likely adsorbent in air ambient is molecular oxygen, which acts as negatively charged surface acceptor after electron capture from the conduction band and thus inducing upward band bending [12, 13]. Under UV-illumination, the photogenerated holes may react with surface acceptors and release the oxidizing agents, which in turn lead to increase of carrier concentration and downward band bending.

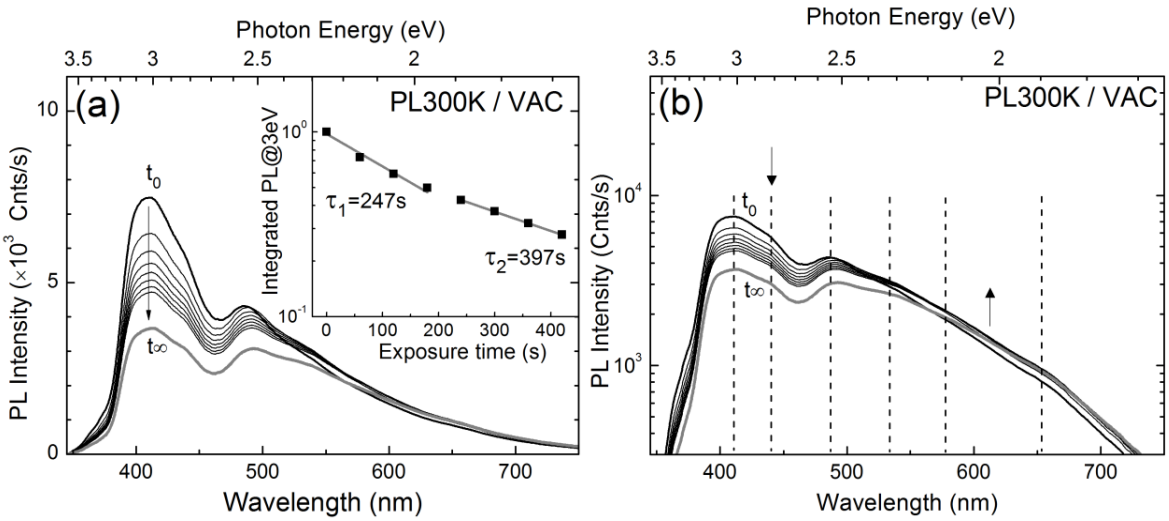

Figure 3. Time evolution of the PL measured from the hybrid ZnO-CNT nanocomposites at 300K in vacuum: (a) time-lapse PL spectra as a function of UV-exposure time. Inset shows decay transient of the integrated PL intensity. (b) Semi-log representation of the PL developments with the main spectral components indicated by vertical dashed markers.

In vacuum at 300K, the overall quantum efficiency is noticeably reduced (~4 fold) compared to that in air ambient (figure 3), as can be seen from the comparison of figures 3 and 2. Since there is no sustained oxygen supply in vacuum, the upward band bending is already reduced due to natural O_2 desorption (without UV-illumination) before the PL measurements even start. It is also noteworthy that the saturated PL spectra, i.e. those measured after prolonged UV-exposures, settle down at very similar levels in the case of air and vacuum, thus only the magnitude of PL changes appears as the decisive distinction. Figure

4 depicts qualitatively similar PL developments observed in vacuum at 10K, except for a considerably higher overall PL quantum efficiency, which is due to suppressed non-radiative recombination pathways at cryogenic temperatures.

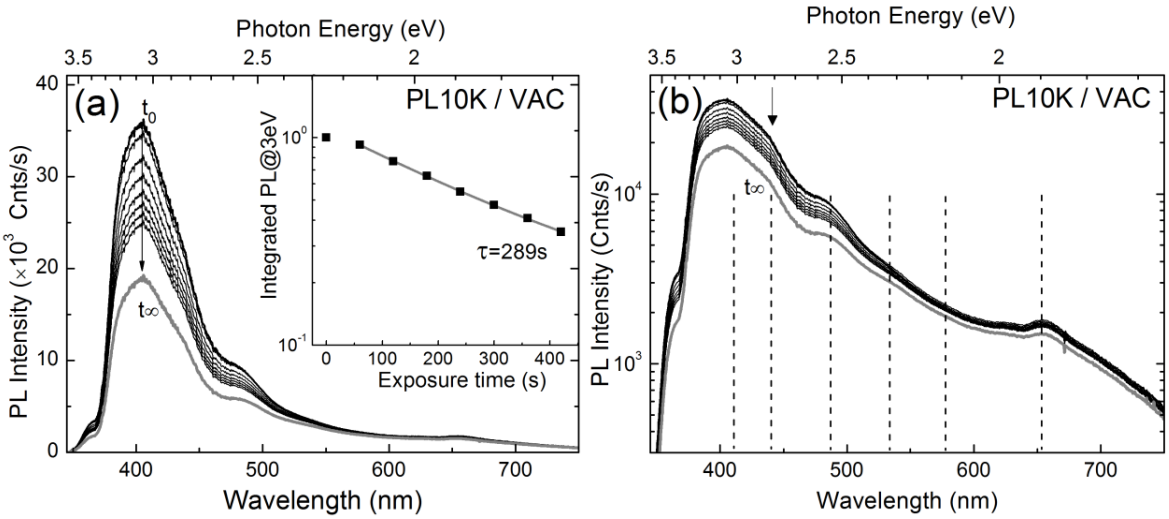

Figure 4. Time evolution of the PL measured from the hybrid ZnO-CNT nanocomposites at 10K in vacuum: (a) time-lapse PL spectra as a function of UV-exposure time. Inset shows decay transient of the integrated PL intensity. (b) Semi-log representation of the PL developments with the main spectral components indicated by vertical dashed markers.

The PL spectra indicate that ZnO nanoparticles are highly defective and are dominated by Zn vacancies. Extended defects formed by these Zn vacancies are rather robust and do not show much variation in the PL excitation-emission experiments performed by varying temperature and ambient. However, the Zn vacancies closer to the surface are greatly affected by ambient and temperature. It is to be noted that at 10K in vacuum the PL spectra lose some amount of intensity over time; this phenomenon is most likely due to charge transfer from ZnO to CNT or due to the band gap states becoming saturated.

4. Conclusion

We have synthesized ZnO-CNT hybrids at 240ºC via non aqueous sol-gel routes. The PL spectra of the ZnO nanoparticles suggest a high level of Zn vacancies in the form of point and extended defects. The Zn vacancies close to the surface, like other surface defects, are very susceptible to the ambient conditions and tend to get dominated by adsorbed oxygen when measured over a period of time. Low temperature PL in vacuum helps in understanding the effect of suppressing the adsorbed oxygen in turn enhancing the PL emission from intrinsic defects which in this present case are mostly V_{Zn}. The observed optical sensitivity of hybrid ZnO-CNT nanocomposites to ambient may lead to new applications as gas sensors.

Acknowledgements

This research has been supported by the European Regional Development Fund project EQUiTANT (F180175TIBT). Research Council of Norway and the University of Oslo through the FUNDAMENT project (No. 251131) is gratefully acknowledged.

References

[1] D Eder 2010 *Chemical Reviews* **110** (3) 1348 https://pubs.acs.org/doi/10.1021/cr800433k
[2] P Rauwel, M Salumaa, A Aasna, A Galeckas, E Rauwel 2016 *Journal of Nanomaterials* 5320625 1 http://dx.doi.org/10.1155/2016/5320625

[3] B J Coppa, C C Fulton, S M Kiesel, R F Davis, C Pandarinath, J E Burnette, R J Nemanich, D J Smith 2005 *J. Appl. Phys.* **97** 103517 https://doi.org/10.1063/1.1898436
[4] E Rauwel, A Galeckas, P Rauwel, M Fleissner Sunding, H Fjellvåg 2011 *J. Phys. Chem. C* **115** (51) 25227 https://pubs.acs.org/doi/abs/10.1021/jp208487v
[5] X L Li, C Li, Y Zhang, D P Chu, W I Milne, H J Fan 2010 *Nanoscale Res. Lett.* **5** 1836 https://doi.org/10.1007/s11671-010-9721-z
[6] J Bae, J B Han, X-M Zhang, M Wei, X Duan, Y Zhang, Z L Wang 2009 *J. Phys. Chem. C* **113** 10379 https://pubs.acs.org/doi/abs/10.1021/jp901011u
[7] E Rauwel, A Galeckas, M Rosário Soares P Rauwel 2017 *J. Phys. Chem. C* **121** 14879 https://pubsdc3.acs.org/doi/abs/10.1021/acs.jpcc.7b03070?journalCode=jpccck
[8] H Zhang, J Sun, C. Liu, Y Wang 2015 *J. Catal.* **331** 57 https://doi.org/10.1016/j.jcat.2015.08.016
[9] A Janotti, C G Van de Walle 2007 *Physical Review B* **76** 165202 https://doi.org/10.1103/PhysRevB.76.165202
[10] H Zeng, Z Li, W Cai, P Liu 2007 *J. Applied Phys.* **102** 104307 https://doi.org/10.1063/1.2803712
[11] M Ghosh, A K Raychaudhuri 2008 *Nanotechnology* **19** 445704 https://doi.org/10.1088/0957-4484/19/44/445704
[12] J W P Hsu, D R Tallant, R L Simpson, N A Missert, R G Copeland 2006 *Applied Physics Letters* **88** 252103 https://doi.org/10.1063/1.2214137
[13] D Wang, N Reynolds 2012 *ISRN Condensed Matter Physics* 950354 1 http://dx.doi.org/10.5402/2012/950354